

Model-Based Bayesian Filtering of Cardiac Contaminants from Biomedical Recordings

R Sameni^{1,2}, M B Shamsollahi² and C Jutten¹

¹ Department of Images and Signals, GIPSA-LAB, INPG, 46 Avenue Félix Viallet, 38031 Grenoble Cedex, France

² Biomedical Signal and Image Processing Laboratory (BiSIPL), School of Electrical Engineering, Sharif University of Technology, Tehran, Iran

E-mail: reza.sameni@gipsa-lab.inpg.fr

Abstract. Electrocardiogram and magnetocardiogram signals are among the most considerable sources of noise for other biomedical signals. In some recent works, a Bayesian filtering framework has been proposed for denoising ECG signals. In this paper, it is shown that this framework may be effectively used for removing cardiac contaminants such as the ECG, MCG, and ballistocardiographic artifacts from different biomedical recordings such as the EEG, EMG, and also for canceling maternal cardiac signals from fetal ECG/MCG. The proposed method is evaluated on simulated and real signals.

Keywords: Model-based filtering, ECG/MCG denoising, EEG denoising, EMG denoising, fetal ECG/MCG extraction. Submitted to: *Physiol. Meas.*

1. Introduction

The electrocardiogram (ECG) is among the strongest bioelectric signals generated in the human body. It is therefore a considerable artifact when we are interested in recording other bioelectric signals such as the electroencephalogram (EEG), electromyogram (EMG), electrogastrogram (EGG), etc. In previous works, many approaches have been proposed for canceling or decreasing such artifacts. However, due to the spatial, temporal, and frequency domain overlap of the ECG with other biopotentials, it is rather difficult to fully remove these artifacts. A similar problem is encountered with the artifacts caused by the ballistocardiogram[‡] (BCG) and the magnetocardiogram (MCG), which are temporally synchronous with the heartbeat.

In a recent work, Bayesian filters such as the *extended Kalman filter* (EKF), *extended Kalman smoother* (EKS), and *unscented Kalman filter* (UKF) were proposed for ECG denoising (Sameni, Shamsollahi, Jutten & Clifford 2007). The state-space model used for these filters was inspired from the work in (McSharry et al. 2003), that suggested the use of Gaussian mixtures to model realistic synthetic ECGs. In (Sameni, Shamsollahi, Jutten & Clifford 2007), a modified version of this model was

[‡] The ballistocardiogram is a record of the body's recoil caused by the cardiac contraction.

used to represent the temporal dynamics of pure ECG, while the noisy ECG recorded from the body surface were considered as noisy observations of the state variables of the dynamical model.

It was later found that by some modifications, the ECG filtering framework developed in (Sameni, Shamsollahi, Jutten & Clifford 2007), could be used as a general framework for removing *cardiac contaminants* (CC) such as the ECG, BCG, and MCG, from other biomedical recordings. This idea has been since implemented and tested over several databases from rather diverse applications, in which conventional CC removal techniques had not led to satisfying results.

In this paper, the details of this general framework are presented, and simulated data are used to quantify its performance. Moreover, several examples from real world applications are presented, on which we have up to now evaluated the method. Due to the variety of the presented applications, the implementation details are skipped and the reader is referred to the Matlab[®] source files and the accompanying technical reports that are online available in the *Open Source ECG Toolbox* (OSET) (Sameni 2006). Note that the proposed method is a filtering framework with several tunable parameters, which enables it to be adapted to different applications. Some general rules are presented throughout the paper, by which the filter parameters can be manipulated and tuned for different situations.

The paper is organized as follows. In section 2, the previously developed ECG filtering framework is reviewed. The details of the proposed extension and a comparison with conventional methods are presented in sections 3 and 4. In section 5, the results on simulated and real data are presented, and the final section is devoted to some discussions and concluding remarks.

2. Review of the Bayesian ECG Filtering Framework

In (Sameni, Shamsollahi, Jutten & Clifford 2007), a nonlinear state-space model was suggested for representing noisy ECG signals recorded from the body surface. The process and observation equations of this model are as follows:

Process equation:

$$\begin{cases} \theta_{k+1} = (\theta_k + \omega\delta) \bmod(2\pi) \\ s_{k+1} = -\sum_{i=1}^N \delta \frac{\alpha_i \omega}{b_i^2} \Delta\theta_i \exp\left(-\frac{\Delta\theta_i^2}{2b_i^2}\right) + s_k + \eta, \end{cases} \quad (1)$$

Observation equation:

$$\begin{cases} \phi_k = \theta_k + u_k \\ y_k = s_k + v_k, \end{cases} \quad (2)$$

where δ is the sampling period, $\Delta\theta_i = (\theta_k - \theta_i) \bmod(2\pi)$, $\omega = 2\pi f$, f is the beat-to-beat heart rate, and N is the number of Gaussian functions used for modeling the shape of the desired ECG. In (1) and (2), θ_k and s_k are assumed as the state variables, and ω , α_i , θ_i , b_i and η are assumed as i.i.d Gaussian random variables considered as process noises.

In the observation equation (2), ϕ_k and y_k are respectively considered as the phase observations and the noisy ECG measurements, and u_k and v_k are the corresponding observation noises. The first observation signal ϕ_k , is a synthetic saw tooth shape signal that is found by detecting the R-peaks of the noisy ECG and linearly assigning

a phase between $-\pi$ and π to the ECG samples between two successive R-peaks. This signal, is in fact a means of modeling the pseudo-periodic behavior of the cardiac dipole as it evolves during the depolarization and repolarization stages of the cardiac cycle.

By defining $\mathbf{x}_k = [\theta_k, s_k]^T$ as the state vector at instant k and $\hat{\mathbf{x}}_k$ as the *posterior* estimate of \mathbf{x}_k , the posterior error of the estimation is defined as $\mathbf{e}_k = \mathbf{x}_k - \hat{\mathbf{x}}_k$ with a covariance matrix $P_k = E\{\mathbf{e}_k \mathbf{e}_k^T\}$. The matrix P_k is an essential part of standard Kalman filter equations and is calculated and updated as the filter propagates in time. The eigenvalues of this matrix can be used to form an *error likelihood ellipsoid* (also known as *concentration ellipsoid* (Van-Trees 2001)) that represents the region of highest likelihood for the true state vector \mathbf{x}_k . This likelihood ellipsoid provides a confidence region for the estimated signals.

The process noise and observation noise vectors of the proposed state-space model are, respectively, defined as follows:

$$\begin{aligned} \mathbf{w}_k &= [\alpha_1, \dots, \alpha_N, b_1, \dots, b_N, \theta_1, \dots, \theta_N, \omega, \eta]^T, \\ \mathbf{v}_k &= [u_k, v_k]^T \end{aligned} \quad (3)$$

All the entries of \mathbf{w}_k and \mathbf{v}_k are assumed as zero-mean random variables. The covariance matrices of the process and observation noises are hence defined as $Q_k = E\{\mathbf{w}_k \mathbf{w}_k^T\}$ and $R_k = E\{\mathbf{v}_k \mathbf{v}_k^T\}$, respectively. An advantage of the Kalman filtering framework is that all the model uncertainties are considered in the entries of the covariance matrices Q_k and R_k . Therefore, we can incorporate the uncertainty of a specific parameter or state variable in (1) and (2), by increasing or decreasing its corresponding entries in Q_k or R_k (Sameni, Shamsollahi, Jutten & Clifford 2007, Gelb 1974, Simon 2006).

The dynamic model proposed in (1), is a nonlinear function of the state and process noise vectors. Therefore, nonlinear extensions of the Kalman filter (KF) such as the EKF, EKS, and UKF are required for estimating the state vector \mathbf{x}_k . In the following sections, for the sake of brevity, we only present the EKS results that were shown to outperform the EKF and UKF in a wide range of signal SNRs (Sameni, Shamsollahi, Jutten & Clifford 2007). Further details concerning this model and the linearized KF equations may be found in (Sameni, Shamsollahi, Jutten & Clifford 2007).

Another important issue in Kalman filtering concerns the stability of the filter. The proof of EKF stability is a challenging and application dependent phenomenon. In (Reif et al. 1999), a set of sufficient conditions have been proposed, under which the estimation error of the discrete EKF is exponentially bounded in mean square with probability one[§]. The required conditions include nonlinear observability rank conditions of the dynamic model, sufficiently small initial estimation errors and sufficiently small observation and process noises. It can be shown that the dynamic model in (1)-(2) satisfies the ranking conditions and the other assumptions proposed in (Reif et al. 1999), for moderate ECG noises. However, the stability bounds which are found by this way are rather conservative and the previous results presented in (Sameni, Shamsollahi, Jutten & Clifford 2007), show that the filter is stable for a wide range of practical SNR scenarios.

[§] At the discrete time index k , the stochastic process ζ_k is said to be exponentially bounded in mean square, if real numbers $\rho, \vartheta > 0$ and $0 < \kappa < 1$ exist such that $E\{\|\zeta_k\|^2\} \leq \rho \|\zeta_0\|^2 \vartheta^k + \kappa$ (Reif et al. 1999).

It should be noted that the dynamical model in (1)-(2) is not limited to ECG signals. In fact, as it is seen in the later presented applications, by using an appropriate mixture of Gaussian kernels, it is possible to filter any pseudo-periodic signal with this model.

3. Cardiac Artifact Removal

The Bayesian filtering framework may further be extended for removing cardiac artifacts from other biomedical signals. For this, it is again supposed that the noisy recordings are $y_k = s_k + v_k$, as defined in (2); but this time we are interested in the residual signal v_k rather than s_k . In other words, s_k represents the CC, while v_k is the signal of interest. Therefore, we can model the CC with the dynamic model in (1) and apply the KF to find an estimate of the artifacts, namely \hat{s}_k . The background signal may then be found as follows:

$$\hat{v}_k = y_k - \hat{s}_k, \quad (4)$$

which is the *innovation* signal of the KF.

The overall filtering procedure is illustrated in Fig. 1 and may be summarized as follows:

- (i) *Baseline wander removal.* For the reliable extraction of the average CC templates, the baseline wander of the noisy records should be removed beforehand.
- (ii) *R-peak detection.* These peaks are required for constructing the phase signal ϕ_k , which is in terms needed for synchronizing the noisy ECG with the dynamic model in (1). They are also used for extracting the mean CC by synchronous averaging over the heart beats. Depending on the power of the CC, as compared with the background signals and noise, the R-peaks may be detectable from the noisy recordings or from any arbitrary ECG channel synchronously recorded with the noisy dataset.
- (iii) *CC template extraction.* Using the R-peaks, the *ensemble average* (EA) and standard deviation of the CC are extracted through synchronous averaging. Several methods have been proposed in the literature for synchronous averaging. One of the most effective approaches in this area is the *Robust Weighted Averaging* method (Leski 2002), which outperforms conventional EA extraction methods and is useful for noisy nonstationary mixtures.
- (iv) *Model fitting.* As proposed in (Sameni, Shamsollahi, Jutten & Clifford 2007, Clifford et al. 2005), by using a nonlinear least square estimation, the parameters of the Gaussian kernel defined in (1) are found, such that the model will best fit the mean CC waveform.
- (v) *Covariance matrix calculations.* The standard deviation of the average CC is used to find the entries of the covariance matrices of the dynamic model noise Q_k , and measurement noise R_k .
- (vi) *Filtering.* Having extracted all the required parameters, the CC may be estimated by the KF framework and the desired background signal is found from (4).

Note further that for online applications or denoising long nonstationary datasets, all of the dynamic model parameters and the covariance matrices may be updated in time by recalculating them from the most recent cardiac beats.

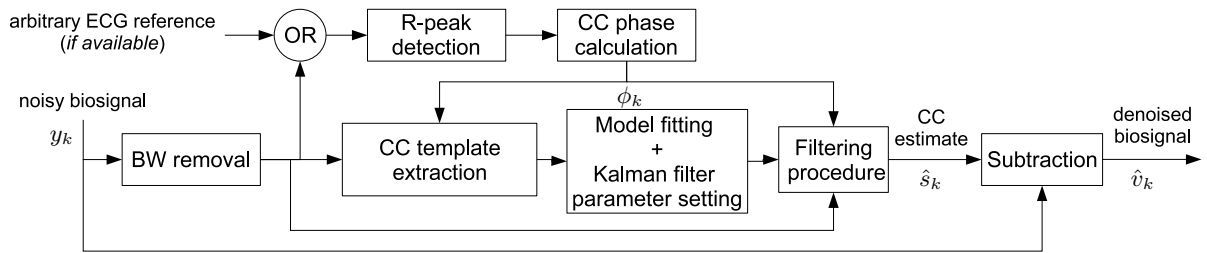


Figure 1. The overall denoising scheme. As shown in this figure the R-peaks of the contaminating signals (CC) may either be detected from an arbitrary reference ECG or from the noisy biosignal after baseline wander (BW) removal.

Table 1. Rules chart for the manipulation of the filter parameters

Situation	Comments
Strong baseline wanders	Remove before Kalman filtering
Low SNR (strong CC)	Decrease the corresponding R_k entries
High SNR (weak CC)	Increase the corresponding R_k entries; additional ECG reference may be required for R-wave detection
Desired signal with highly colored spectrum	Remove the baseline wander as much as possible
Desired signal highly nonstationary	Allow the filter to adaptively change R_k using the KF innovation signal
Irregular CC (high inter-beat variations of CC)	Increase the corresponding Q_k entries
Desired signal highly non-Gaussian	Better performance may be achieved using UKF
Batch offline processing	EKS outperforms EKF
Online processing	Use EKF or fixed-lag EKS with a single heart beat delay for parameter estimation

A rather general algorithm for selecting the filter parameters was presented in (Sameni, Shamsollahi, Jutten & Clifford 2007). Some other rules-of-thumb are summarized in Table 1, by which the original filter parameters can be adapted to different situations.

4. Bayesian Filtering versus Conventional Techniques

Cardiac signal processing is a highly developed and competitive area that might raise suspicions about the effectiveness of the proposed method. However, we can argue that this method is in fact a generalization of conventional denoising techniques.

In fact, from a filtering point of view, Kalman filters can be assumed as *adaptive filters* that continuously move the location of the poles and zeros of their transfer functions, according to the signal/noise content of the input signal and the prior model of the signal dynamics. This feature, allows the filter to adapt with different spectral shapes and temporal non-stationarities. The method is therefore more general than other frequency domain filters such as FIR, IIR, and Wiener filters that use a fixed pole-zero configuration in their transfer function.

A similar argument holds about *wavelet denoising* (WD) (Kestler et al. 1998), as it performs a sort of ‘blind thresholding’ between the signal and noise, without using the

temporal structure and pseudo-periodicity of the cardiac contaminants. The proposed method may nevertheless be linked with the known WD techniques, by applying the Bayesian filter in the wavelet domain rather than the original time domain.

As explained in the previous section, since the ensemble average (EA) of the CC is required for training the KF parameters, the proposed method is also comparable with conventional EA removal techniques that simply remove the EA of the contaminating signals from the noisy recordings (Allen et al. 1998). The proposed method is again more general in the sense that it adaptively changes its ensemble average template, accounting for the inter-beat variations of the CC. In fact, in the extreme case that the desired signal is very clean (with low cardiac contamination), since the KF is seeking for the CC that is highly defected by the background signal, the observation signal of the KF is not ‘trusted’, and the filter will follow its dynamic model that was trained by the EA of the CC. Mathematically speaking, in this case, the entries of the observation noise covariance matrix R_k are large and the Kalman gain is small (Kay 1981). The proposed method therefore reduces to simple EA subtraction. On the other hand, for extremely noisy signals (with high cardiac contamination), the R_k entries will be rather small and the filter will ‘trust’ the observations for CC estimation. Therefore, the filter fully tracks the CC within the input signal.

Hence, the Bayesian approach theoretically outperforms many of the conventional techniques, in the same manner that model-based parametric methods typically outperform nonparametric methods, as long as their underlying model is consistent (Candy 2005). However, due to the broadness of the possible applications, it is not possible to prove this claim in the general case, and case-by-case quantitative studies are required for different applications. In the following, we present the results of the proposed method on simulated data and typical results that were achieved in several diverse applications, for which, conventional denoising methods did not yield to satisfying results.

5. Applications

In this section, the performance of the proposed method is studied on simulated and real data. For simulated data, the SNR improvement $\|$ is used as a measure of performance. For real data, it is not possible to calculate the SNR improvement. However, in order to have a quantitative measure of performance, we propose to compare the amount of ‘periodicity’ of the signal before and after CC removal. Here, the idea is that an artifact-free signal should not contain any waveform that is synchronous with the ECG signal. Based on this idea, we first find the ECG R-peaks and the phase ϕ_k , as explained in section 2. Then by using ϕ_k , each sample of the signal is compared with its *dual sample*, which is a sample in the successive ECG beat having the same phase value. We can define τ_k as the time distance between the sample k and its dual sample, which is formally defined as follows:

$$\tau_k = \min\{\tau | \phi_{k+\tau} = \phi_k, \tau > 0\} \quad (5)$$

Using this definition, the following correlation coefficient is proposed as an overall *periodicity measure* (PM) for a signal x_k :

$$\text{PM} = |\text{corrcoef}(x_k, x_{k+\tau_k})| = \frac{|E\{x_k x_{k+\tau_k}\}|}{|E\{x_k^2\}E\{x_{k+\tau_k}^2\}|^{1/2}} \quad (6)$$

$\|$ The SNR improvement is the output SNR, in decibels(dB), minus the input SNR, in dB.

where $E\{\cdot\}$ represents averaging over the time index k . From this definition $0 \leq \text{PM} \leq 1$, where $\text{PM} = 0$ indicates an aperiodic signal, and $\text{PM} = 1$ indicates a fully periodic one. An effective CC filter should be able to remove any component that is temporally synchronous with the heartbeat and the samples x_k and $x_{k+\tau_k}$ should become uncorrelated; resulting in a PM close to zero. It should of course be noted that the reduction of PM is a *necessary* but not a *sufficient* measure of the filtering performance. In fact, the PM might be reduced, e.g. by an increase of the overall noise, without an improvement of the signal quality. Therefore, other evidence such as the visual inspection of the resultant waveforms or a comparison of the signal spectra before and after filtering is always required besides this measure.

5.1. Simulated Data

The application domain of the proposed method is rather vast, ranging from low amplitude EEG to nonstationary EMG. In these applications, the signal SNR and spectral color of the *target signal* are very different. Therefore, in order to show the applicability of the proposed method in these applications, we can use spectrally colored signals to simulate arbitrary signals representing the EEG or EMG. Then by diluting this target signal with ECGs (or simulated ECGs) in different strengths, noisy signals are achieved that may be used for performance studies. For illustration, in Fig. 2(a) a thirty second segment of an arbitrary signal with a frequency range of below 25Hz and a $1/f$ spectral shape is depicted. This signal was diluted with a rather clean ECG, such that its SNR reduced to 7.6dB. The resultant signal, depicted in Fig. 2(b), was then denoised by the EKS. The denoised signal can be seen in Fig. 2(c). In this example, the output SNR was increased to 15.1dB using the proposed method. The PM factors of the original, noisy, and denoised signals were 0.095, 0.179, and 0.074, respectively.

For a consistent quantitative study, *Monte Carlo* simulations were carried out with different input signals and by sweeping the SNR and spectral color of the target signal over the entire range of their practical values. There are different ways of generating spectrally colored signals (Kay 1981), and realistic biosignals (Sameni, Clifford, Jutten & Shamsollahi 2007). For the current study, we adopt the method previously reported in (Sameni, Shamsollahi, Jutten & Clifford 2007), i.e., we model the signal color by a single parameter representing the slope of a spectral density function that decreases monotonically with frequency:

$$S(f) \propto \frac{1}{f^\beta}, \quad (7)$$

where f is the frequency and β is the noise color parameter. *White noise* ($\beta = 0$), *pink noise* ($\beta = 1$) or *flicker noise*, and *brown noise* ($\beta = 2$) or the *random walk process*, are three of the most commonly referenced noises.

In practice, in order to generate colored noise following (7), samples of white noise are generated and transferred into the frequency domain using the *discrete Fourier transform* (DFT). Then, by altering the frequency components of the DFT according to (7), and transferring the reshaped DFT back to the time-domain, typical samples of spectrally colored signals are realized. This procedure was used to simulate the target signals of interest.

On the other hand, for simulating the cardiac artifacts, the MIT-BIH Normal Sinus Rhythm Database (Goldberger et al. 2000 (June 13), *The MIT-BIH Normal*

Sinus Rhythm Database n.d.) was used. This database has a sampling rate of 128Hz. From this database 20 low-noise segments of 30 seconds ECG without considerable artifacts were visually selected from different channels. Next, normalized portions of these segments were added to the simulated target signals to achieve simulated signals in different SNRs. These signals were next filtered by the proposed method. In high SNRs, in which the ECG peaks were not detectable from the noisy signal, the required R-peak detection was performed on the original ECG. This is equivalent to using an arbitrary reference ECG channel in Fig. 1.

The overall simulation procedure was repeated 10 times for each of the 20 ECG segments, in different SNRs and with different spectrally colored target signals. The input SNR was swept in the range of -20dB to 20dB, in 5dB steps, and the signal spectral parameter β was swept in the range of 0 (white noise) to 2.5 (beyond brown noise), in 0.2 steps. This range of parameters is believed to be sufficient for simulating practical scenarios (c.f. (Malmivuo & Plonsey 1995) for some typical spectral curves).

The SNR improvement achieved by the proposed filtering procedure was finally averaged over the 200 results (20 ECG segments \times 10 trials). The result of this study is depicted in Fig. 3. This result shows an SNR improvement surface, continuously changing according to the input SNR and spectral color. It is seen that the SNR

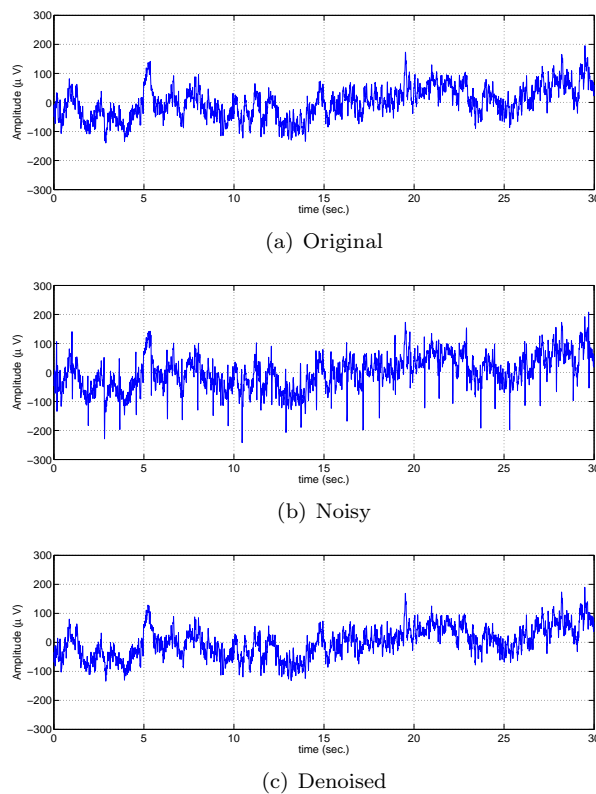


Figure 2. Results of the EKS on a mixture of simulated signal plus ECG artifacts. The (a) original, (b) noisy, and (c) denoised signals can be seen in this figure. The SNR of the noisy signal was improved from 7.6dB to 15.1dB using the EKS.

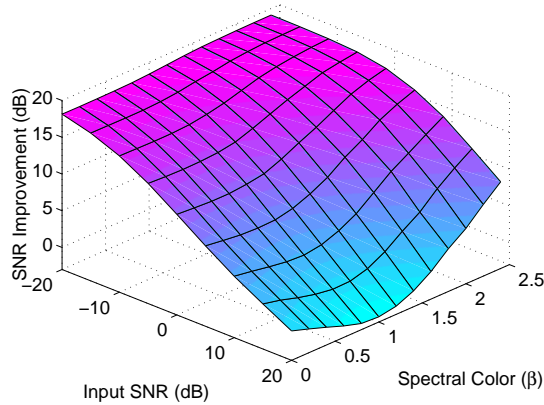


Figure 3. SNR improvement results achieved on simulated data in different input SNRs and different spectral colors.

improvement is generally better in low SNRs than in high SNRs. This was already expected, since in high input SNRs there is not very much of CC to be removed by the filter. The SNR improvement also generally increases as the signal spectrum becomes more colored. This is partially due to the fact that a high spectral color corresponds to a high β value in (7), representing a narrow-band signal. According to the filtering scheme in Fig. 1, such components are not affected by the KF, as they are bypassed by the BW removal block. However, in Fig. 3 it is interesting to see that in input SNRs above 5dB, a minimum SNR improvement is achieved for $\beta \approx 1$, i.e. for a target signal having a pink spectrum. This can be explained by considering the KF as an adaptive filter that adaptively changes its input-output transfer function in the frequency domain, to separate the signal from noise. This separation becomes more difficult, when the target signal and the CC have similar spectral shapes. Therefore, the minimum performance around $\beta = 1$ indicates that the CC used in our Monte Carlo simulations were spectrally closer (on average) to a pink spectrum than other spectral shapes. Therefore, the filtering of the CC has been most difficult for $\beta \approx 1$, leading to smaller SNR improvements at the filter output.

Practical target signals do not usually have a monotonically decreasing spectrum. However, from the Monte Carlo simulations in Fig. 3, the approximate performance of the proposed method may be roughly predicted for different applications, depending on the SNR and spectral color of the target signal.

The PM, defined in (6), was also calculated for the baseline wander removed simulated data, before and after the filtering procedure. As explained before, an effective CC removal should decrease PM (although not being a sufficient measure of performance). This can be seen in the results shown in Fig. 4. Note however that from Fig. 4(a) it is seen that in high input SNRs and low spectral colors (target signal close to white noise), the input PM is already rather low and the filter does not decrease it more. Nevertheless, the output PM is always less than the input PM.

It should also be noted that results of Figs. 3 and 4 are an underestimate of the actual performance, since for these simulations the KF parameters were all selected in an automated way from the noisy signals, while in real applications (especially in offline processing) we can always fine-tune the parameters for the specific signal.

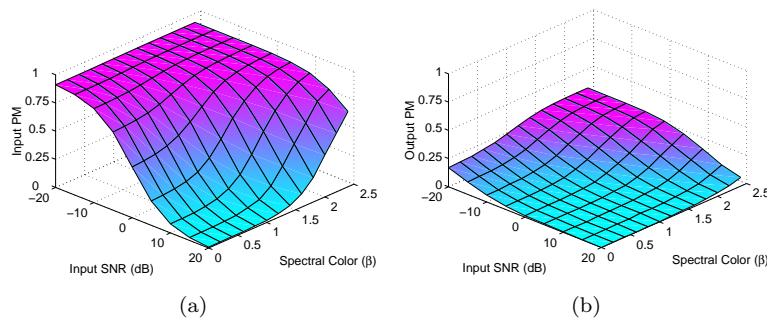


Figure 4. Periodicity measures (PM) achieved on simulated data in different input SNRs and different spectral colors, (a) before and (b) after denoising. The decrease of PM is used as a necessary, but not sufficient, measure of the filtering performance.

5.2. EEG Denoising

The effective removal of cardiac artifacts such as the ECG, MCG, and the BCG artifacts from EEG and MEG recordings, remains a challenging issue. The conventional method of CC cancellation, is to subtract the *ensemble average* (EA) of the CC, either directly or adaptively from the noisy brain recordings (Strobach et al. 1994, Allen et al. 1998, Allen et al. 2000). However EA subtraction is not enough because it does not account for inter-beat variations of the cardiac waveforms. More effective means of EEG denoising are KF based approaches that use additional channels such as the electrooculogram (EOG) (In et al. 2006), or a motion channel attached to the temporal artery (Bonmassar et al. 2002), for recording the BCG and motion artifacts. In these works, the CC of the EEG has been approximated by a linear mixture of the EOG or an artery channel, and the weights of the mixture have been estimated by a KF. The drawback of these approaches is that they require additional EOG or reference artery channels. Moreover, due to the three-dimensional propagation of the cardiac potentials, the CC recorded from different leads can not be reconstructed from a linear mixture of a single reference channel, unless the reference channel is recorded from a location close to the distorted channel, or alternatively, multiple reference channels are used. Both of these methods are practically limiting and do not fully remove the artifacts. A comparative study of the different methods may be found in (Grouiller et al. 2007). Other methods, based on wavelet transforms and nonlinear noise reduction (Wan et al. 2006), and independent component analysis (Srivastava et al. 2005, Mantini et al. 2007), have also been proposed.

With this background, the method explained in previous sections was used for removing CC from EEG signals recorded during an fMRI experiment. In this case, the CC of the EEG can be considered as a mixture of ECG and BCG signals. The presented method may be considered as an extension of the work presented in (Strobach et al. 1994, In et al. 2006, Bonmassar et al. 2002). The privilege of the proposed method over these previous approaches is that the overall shape of the contaminating ECG plus BCG is extracted from the noisy EEG channel itself, without the need of any reference BCG channels or lead projections. Next, by using the extracted waveform, the artifacts are removed by an EKF or EKS. Note that in the proposed method, a single ECG channel is also required for R-peak detection,

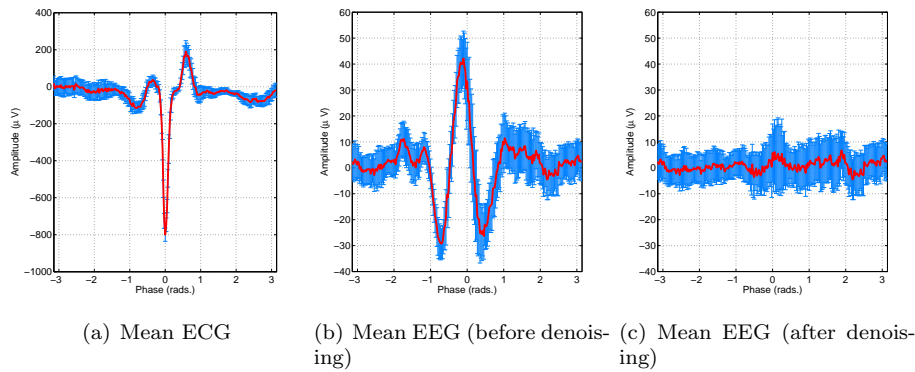


Figure 5. The average and SD-bars of the (a) ECG, (b) EEG before denoising, and (c) EEG after denoising, by synchronous averaging of the data using the ECG R-peaks.

which can be simultaneously recorded from any arbitrary ECG lead.

This idea was tested on a dataset consisting of an EEG channel recorded from the standard AF_8 lead of an awake subject in rest condition with closed eyes, during an fMRI experiment[¶]. An arbitrary ECG channel was also simultaneously recorded from the subject. The sampling rate of the dataset was 250Hz. Visually inspecting the data, the EEG appeared to have considerable artifacts that were temporally synchronous with the ECG beats. These artifacts are clearly seen in the EEG channel depicted in Fig. 6(b). In order to remove the CC, the single ECG channel was used to localize the artifacts within the EEG recordings. For this, the baseline wander of the raw data was removed and the R-peaks of the ECG were detected from the ECG channel. In this example a two-stage median filter, with 200ms and 600ms window lengths, was used for baseline wander removal. Next, by using the R-peak information, the baseline removed EEG channels were synchronously averaged over the ECG period and the average and standard deviation of the ECG beat template were extracted. This gave the average shape of the CC (ECG plus BCG) that were contaminated over the EEG. The resultant mean and standard deviation bars can be seen in Fig. 5, for the reference ECG channel and the EEG before and after filtering. As we see, the CC of the EEG in Fig. 5(b), seem to be smoothed by the fMRI magnetic field and do not resemble the reference ECG in Fig. 5(a). This means that conventional adaptive noise cancellation ideas that remove linear mixtures of three orthogonal ECG leads from the EEG channels are not applicable to this data.

Next, using the average CC template, the parameters of the Gaussian mixtures required for the EKS were extracted according to the steps described in section 2. Finally, by applying the EKS to the noisy EEG recording, the CC was estimated from the background EEG. The noise free EEG signal was achieved by subtracting the estimated CC from the original noisy recording. In Fig. 6, a typical segment of the resultant EEG is plotted versus the original AF_8 channel. As it can be seen, the EKS has effectively removed the CC from the EEG channel. The periodicity measure defined in (6), was 0.42 for the original AF_8 channel, 0.07 using the conventional EA

[¶] The EEG recordings used in this section have been provided by Dr. Christophe Phillips from the Cyclotron Research Centre, Liege, Belgium.

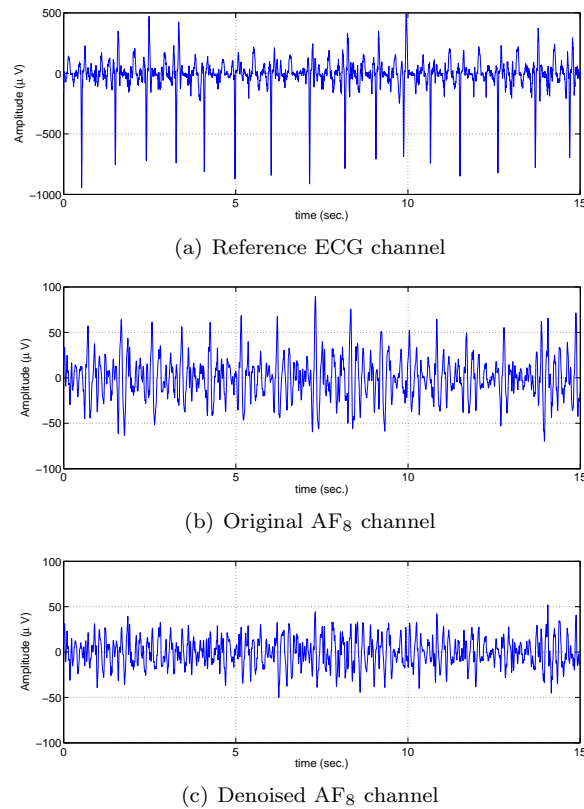


Figure 6. Results of the proposed method on a segment of EEG signals recorded during an fMRI experiment. (a) Reference ECG channel, (b) Noisy AF₈ EEG channel, (c) AF₈ channel after ECG removal.

subtraction method, and 0.04 after applying the proposed method. Even though the PM values of conventional EA subtraction and the proposed method are rather close, the proposed method was found to be more robust to inter-beat deviations of the cardiac signals.

The spectral density function of the original and denoised EEG signals are depicted in Fig. 7. As it is seen, the filtering procedure has changed the spectrum in the *theta* and *alpha* bands, which are important frequency bands of the EEG spectrum. This implies that spectral analysis of the EEG without CC removal can be rather misleading.

Another example is presented in Fig. 8, for an EEG segment of the MIT-BIH Polysomnographic Database, recorded during sleep from the C₄-A₁ channel, with a sampling rate of 250Hz (*MIT-BIH Polysomnographic Database* n.d.). From this figure, we can again notice that the CC peaks that were synchronous with the ECG R-peaks have been effectively removed, while the non-ECG contents and the alpha rhythms have been preserved. The PM of the noisy and denoised signals were 0.15 and 0.001, respectively. The noisy and denoised signal spectra are also compared in Fig. 9, where we can see that the signal spectrum has been considerably changed after CC removal, especially in the beta band and higher frequencies.

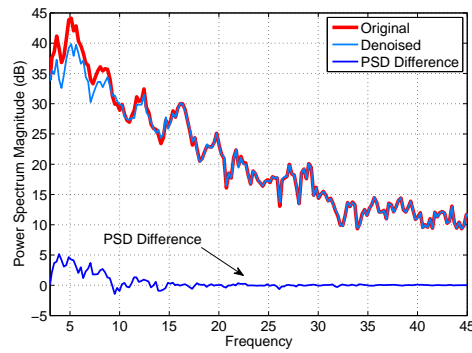
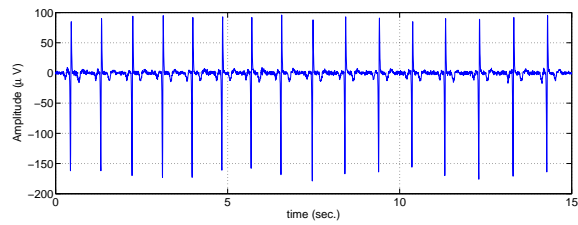
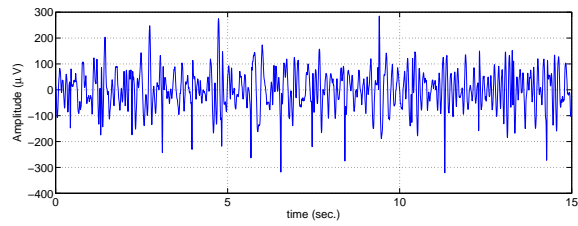


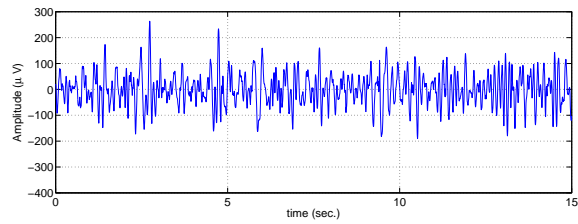
Figure 7. The spectral estimate of the original and denoised EEG signals, from the fMRI experiment data. The difference of the two spectra is plotted at the bottom.



(a) Reference ECG channel



(b) Original EEG channel



(c) Denoised EEG channel

Figure 8. Results of the proposed method on a segment of EEG signals from the MIT-BIH Polysomnographic Database. (a) Reference ECG channel, (b) Noisy C_4-A_1 EEG channel, (c) C_4-A_1 channel after ECG removal.

5.3. Fetal ECG Extraction

The fetal ECG recorded from the maternal abdomen, and more recently the MCG, are the two common noninvasive means of fetal cardiac signal recording. However, these

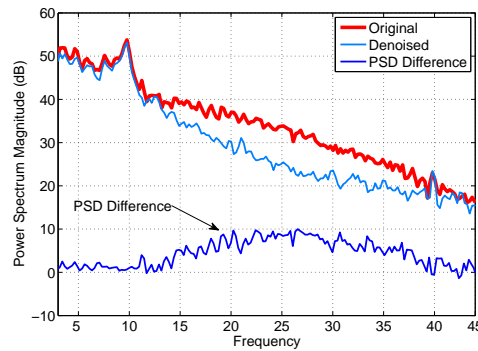


Figure 9. The spectra of the original and denoised EEG signals, from the MIT-BIH Polysomnographic Database. The difference of the two spectra is plotted at the bottom.

recordings are heavily contaminated with maternal ECG or MCG, which depending on the gestational age and electrode locations, can be up to ten to thirty times stronger than the fetal components. A classical method of maternal ECG removal is the adaptive noise canceler and its extensions (Widrow et al. 1975), which do not fully remove the maternal artifacts. A more effective means of removing these contaminants is to use blind or semi-blind source separation techniques such as ICA (De Lathauwer et al. 2000, Sameni et al. 2006). In this case, the maternal and fetal ECGs are assumed to form two independent subspaces and ICA (or more generally Independent Subspace Analysis (Cardoso 1998)) tends to separate these two subspaces. However, these methods require multiple channels, and in presence of noise or with special lead configurations, the subspaces of the fetal and maternal cardiac signals are not fully separated by linear ICA, which results into fetal signals that are still contaminated by the maternal components.

The proposed Bayesian filtering framework can therefore be rather effective for removing the maternal artifacts. Following the filtering procedure mentioned in section 2, the EKS may be set up to find the best estimate of the maternal signals from each of the ECG or MCG channels. In this case, the fetal components and other noises and artifacts are considered as noise for the maternal signals. The EA of the maternal ECG may be extracted from the R-peaks of the maternal ECG within a single channel recording, or from an arbitrary maternal ECG or MCG reference channel. Next, by removing the estimated maternal signals from the original recordings, the fetal signals plus noises, other than the maternal ECG, are achieved. Depending on the SNR of the recordings, the fetal components may be directly detectable from the residual signals, or a post-processing such as a secondary KF trained over the fECG/fMCG or a wavelet denoiser might be required to extract them from the remaining background noise.

To illustrate, an ECG signal recorded from the maternal abdomen is depicted in Fig. 10(a). This signal has been taken from the DaISy database (De Moor n.d.), having eight channels and a sampling rate of 250Hz. The proposed method was applied to the first channel of this dataset for removing the maternal ECG. The residual signal containing the fetal ECG and background noise is seen in Fig. 10(b).

As a benchmark approach, the ICA denoising approach proposed in (Jung

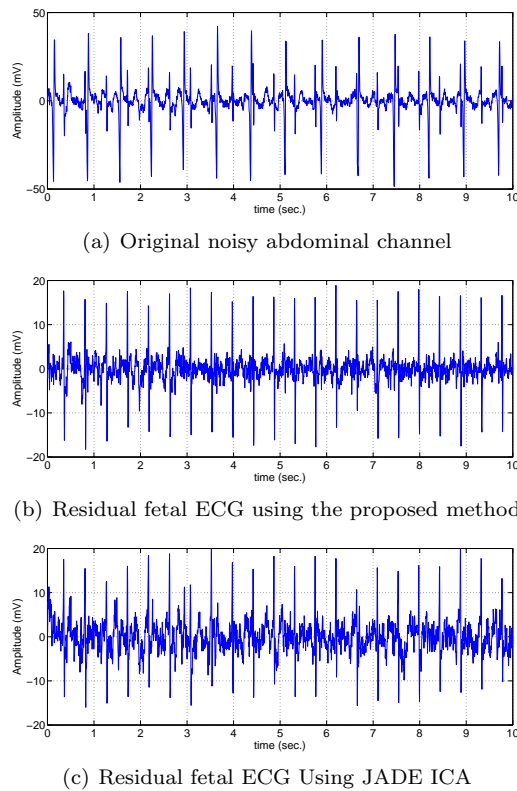


Figure 10. Results of the proposed method and a classical ICA denoising method on a segment of maternal abdominal signals containing maternal and fetal ECGs.

et al. 2000), was also applied to the the DaISy dataset. For this, the eight channels were decomposed into eight independent components by using the JADE ICA algorithm (Cardoso n.d.). Four of the extracted components clearly corresponded to the maternal ECG, two components to the fetal ECG, and the other two were mainly noise with some minor traces of the fetal R-waves. In order to cancel the effect of maternal ECG, the first four components were set to zero and the rest of the channels were remixed together to achieve the maternal ECG free signals. One of the denoised ECG channels (corresponding to the same channel used by the KF approach in Fig. 10(b)), is depicted in Fig. 10(c). From this figure it can be seen that the single channel KF outperforms ICA denoising which used the information within all the eight channels. Quantitatively, the PM of the original noisy signal, the ICA denoised signal, and the KF denoised signal were 0.84, 0.23, and 0.09, respectively.

In some related studies, it was also experienced that depending on the configuration of the maternal abdominal array and the fetal gestational age and position, it sometimes happens that the maternal and fetal subspaces are not separable by any linear transform, including ICA and its extensions. However, even in these cases the proposed method, which performs a nonlinear filtering, is able to remove the maternal signals from the fetal recordings.

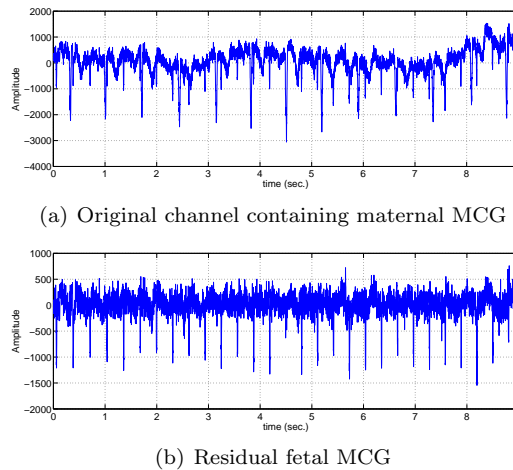


Figure 11. Results of the proposed method on MCG recordings containing maternal and fetal MCGs.

5.4. Fetal MCG Extraction

The next example consists of MCG signals recorded by a SQUID Biomagnetometer system, from a pregnant woman with a sampling rate of 1000Hz using a filtering bandpass between 0.3Hz and 500Hz⁺. The pregnant woman was positioned *supine*, i.e., with a slight twist to either side, to prevent compression of the inferior *vena cava* by the pregnant uterus. The dewar was positioned with its curvature above the fetal heart after sonographic localization as close to the maternal abdominal wall without contact as possible (Grimm et al. 2003). The dataset are however highly contaminated with maternal MCG. The results of removing the maternal CC from a typical segment of these signals using the proposed method are depicted in Fig. 11. The PM before and after maternal MCG cancellation were 0.55 and 0.02, respectively.

5.5. EMG Signal Denoising

Another tested application of the proposed method was the removal of ECG contaminants from diaphragmatic EMG signals recorded from an *intraoesophageal* electrode*. In this application we were interested in the extraction of diaphragmatic EMG bursts synchronous with the respiration. The exact detection of the beginning and ending points of the EMG burst are widely used in respiratory studies. However, the recorded EMG are usually highly contaminated with ECG. The conventional method for removing such artifacts is to detect the QRS-segments of the ECG and to remove their EA or to directly set them to zero. This however removes considerable portions of the EMG signal and causes spurs in the EMG spectrum.

For this example, the procedure was similar to the previous examples. Since the CC was strong, the R-peaks of the ECG were directly estimated from the noisy

⁺ The MCG recordings used in this section have been provided by Dr. Dirk Hoyer from the Biomagnetic Center of the Department of Neurology, Friedrich Schiller University, Jena, Germany.

* The EMG recordings used in this section have been provided by Dr. Vincent Vigneron from the Laboratory of Informatique, Biologie Intégrative et Systèmes Complexes (IBISC), CNRS FRE 2873, Evry, France.

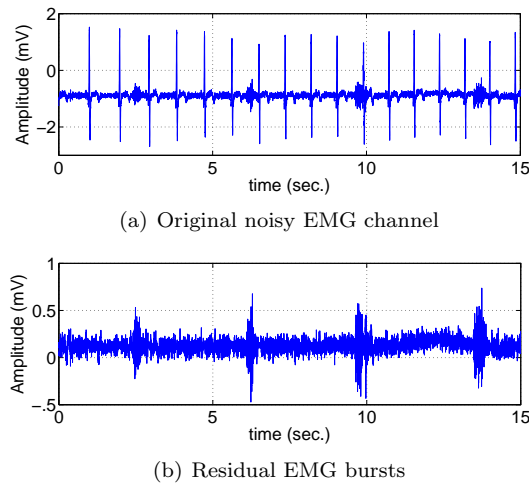


Figure 12. Results of the proposed method on EMG recordings highly contaminated with ECG.

recording, from which the ECG EA was calculated. Next, the dynamic model parameters were selected according to the EA of the ECG artifacts and the EKS was applied to the noisy recordings. After estimating the ECG and removing it from the original recordings, the residual signal contains the desired diaphragmatic EMG. For this application, due to the nonstationary nature of EMG bursts, the adaptive modification of the measurement noise variance proposed in (Sameni, Shamsollahi, Jutten & Clifford 2007), was used. This procedure is based on the monitoring of the KF innovation signal, allowing the filter to adapt the KF measurement noise variance R_k , according to the noise contents of the signal, such that the innovation signal becomes spectrally white \ddagger .

An example of an EMG burst signal denoised with this approach is depicted in Fig. 12. In this example, the PM before and after ECG cancellation were 0.68 and 0.002, respectively. The resultant signal may be further used for EMG burst analysis and depending on the quality of the recorded signals, additional post-filtering may be required to reject the out-of-band noise.

6. Discussion and Conclusion

In this paper, a model-based Bayesian filtering framework was presented for removing cardiac contaminants from various biomedical signals. It was shown that the method is applicable to as few as single channel recordings with an arbitrary reference ECG/MCG channel for R-peak detection.

In summary, the proposed method can be considered as a filter that gives the best minimum mean square estimate of the CC based on *a priori* knowledge of the pseudo-periodic nature of the ECG, MCG, or the BCG. This method is hence using the temporal and frequency domain information about the CC. Nevertheless, when

\ddagger Note that in the KF context, the whiteness of the innovation signal implies that all the information concerning the estimated process, up to the second order statistics, have been extracted from the observation signal.

multichannel recordings are available, one can use the additional information provided by the spatial diversity of the sensors, which is the essence of spatial filtering methods used in *blind source separation*. From this point of view, the proposed filtering framework and source separation techniques, such as ICA, may be jointly used to discriminate the CC simultaneously in time, frequency and space. For example, for the fetal ECG extraction problem presented in section 5.3, a simple realization of this idea would be to decompose the multichannel recordings into statistically independent components, apply the KF to the extracted components, and to recompose the components to achieve the denoised multichannel recordings. This extension can especially be useful for the cases, in which the maternal and fetal QRS complexes overlap with each other and the single channel KF approach may fail to extract the fetal components.

For the sake of brevity, the presented results were only based on the EKS. However, other types of Bayesian filters such as the UKF and the *particle filter* (PF) can be used in the same manner for highly nonlinear and non-Gaussian noise scenarios (Haykin 2001).

Due to the recursive structure of the KF, the proposed method is also computationally efficient and of special interest for real-time applications. Generally, the computation time of this method is linearly proportional to the signal length in samples. For the currently developed Matlab[®] source codes (available at (Sameni 2006)) the computation time is already close to real-time on a 3GHz CPU for signals with a sampling rate of up-to 1kHz (except for the CC template fitting step of the algorithm that is carried out by the user through an interactive graphical user interface, which allows the user to adjust the number and locations of the Gaussian kernels). However, these Matlab[®] codes may be further optimized and converted into low-level languages for being used in pre-processing units of clinical monitoring systems.

Acknowledgment

This work was partially supported by Iran Telecommunication Research Center (ITRC), the French Embassy in Iran (PAI Gundishapur), and by the Center for International Research and Collaboration (ISMO) in Iran.

The authors would also like to thank Dr. Christophe Phillips from the Cyclotron Research Centre, Liege, Belgium, for providing the EEG recordings, Dr. Dirk Hoyer from the Biomagnetic Center of the Department of Neurology, Friedrich Schiller University, Jena, Germany, for providing the MCG recordings, and Dr. Vincent Vigneron from the IBISC Laboratory, CNRS FRE 2873, Evry, France, for providing the EMG recordings.

References

- Allen P J, Josephs O, & Turner R 2000 *Neuroimage* **12**(2), 230–239.
 Allen P J, Polizzi G, Krakow K, Fish D R & Lemieux L 1998 *Neuroimage* **8**(3), 229–239.
 Bonmassar G, Purdon P L, Jaaskelainen I P, Chiappa K, Solo V, Brown E N & Belliveau J W 2002 *NeuroImage* **16**(4), 1127–1141.
 Candy J V 2005 *Model-Based Signal Processing* Wiley-IEEE Press.
 Cardoso J F 1998 in 'Proceedings of the IEEE International Conference on Acoustics, Speech, and Signal Processing (ICASSP '98)' Vol. 4 pp. 1941–1944.
 Cardoso J F n.d. *Blind Source Separation and Independent Component Analysis*.
 *<http://www.tsi.enst.fr/~cardoso/guidesepsou.html>

- Clifford G D, Shoeb A, McSharry P E & Janz B A 2005 *International Journal of Bioelectromagnetism* **7**(1), 158–161.
- De Lathauwer L, De Moor B & J. V 2000 *IEEE Trans. Biomed. Eng.* **47**, 567–572.
- De Moor B n.d. *Database for the Identification of Systems (DaISy)*.
*<http://homes.esat.kuleuven.be/~smc/daisy/>
- Gelb A, ed. 1974 *Applied Optimal Estimation* MIT Press.
- Goldberger A L, Amaral L A N, Glass L, Hausdorff J M, Ivanov P C, Mark R G, Mietus J E, Moody G B, Peng C K & Stanley H E 2000 (June 13) *Circulation* **101**(23), e215–e220. *Circulation Electronic Pages*: <http://circ.ahajournals.org/cgi/content/full/101/23/e215>.
- Grimm B, Haueisen J, Huottilainen M, Lange S, Leeuwen P V, Menendez T, Peters M J, Schlessner E & Schneider U 2003 *Pacing Clin. Electrophysiol.* **26**, 2121–2126.
- Grouiller F, Vercueil L, Krainik A, Segebarth C, Kahane P & David O 2007 *NeuroImage* **38**(1), 124–37.
- Haykin S, ed. 2001 *Kalman Filtering and Neural Networks* John Wiley & Sons Inc.
- In M H, Lee S Y, Park T S, Kim T S, Cho M H & Ahn Y B 2006 *Physiological Measurement* **27**(11), 1227–1240.
*<http://stacks.iop.org/0967-3334/27/1227>
- Jung T, Humphries C, Lee T, McKeown M, Iragui V, Makeig S & Sejnowski T 2000 *Journal of Psychophysiology* **37**, 163–178.
- Kay S M 1981 *Proc. IEEE* **69**, 480–481.
- Kestler H A, Haschka M, Kratz W, Schwenker F, Palm G, Hombach V & Höher M 1998 in ‘Proceedings IEEE Conference on Computers in Cardiology’ pp. 233–236.
- Leski J 2002 *IEEE Trans. Biomed. Eng.* **49**(8), 796–804.
- Malmivuo J A & Plonsey R, eds 1995 *Bioelectromagnetism, Principles and Applications of Bioelectric and Biomagnetic Fields* Oxford University Press.
*<http://butler.cc.tut.fi/~malmivuo/bem/bembook>
- Mantini D, Perrucci M, Cugini S, Ferretti A, Romani G & Gratta C D 2007 *Neuroimage* **34**(2), 598–607.
- McSharry P E, Clifford G D, Tarassenko L & Smith L A 2003 *IEEE Trans. Biomed. Eng.* **50**, 289–294. *MIT-BIH Polysomnographic Database* n.d.
*<http://www.physionet.org/physiobank/database/slpdb/>
- Reif K, Gunther S, Yaz E & Unbehauen R 1999 *IEEE Trans. Automat. Contr.* **44**(4), 714–728.
- Sameni R 2006 *Open Source ECG Toolbox (OSET)*.
*<http://ecg.sharif.ir/>
- Sameni R, Clifford G D, Jutten C & Shamsollahi M B 2007 *EURASIP Journal on Advances in Signal Processing* **2007**, Article ID 43407, 14 pages. ISSN 1687-6172, doi:10.1155/2007/43407.
*<http://www.hindawi.com/GetArticle.aspx?doi=10.1155/2007/43407>
- Sameni R, Jutten C & Shamsollahi M B 2006 in ‘Proc. of the International Symposium on Signal Processing and Information Technology (ISSPIT’06)’ Vancouver, Canada pp. 656–661.
- Sameni R, Shamsollahi M B, Jutten C & Clifford G D 2007 *IEEE Trans. Biomed. Eng.* **54**(12), 2172–2185.
- Simon D, ed. 2006 *Optimal State Estimation* John Wiley & Sons Inc.
- Srivastava G, Lau S C H K, Glover G & Menon V 2005 *Neuroimage* **24**(1), 50–60.
- Strobach P, Abraham-Fuchs K & Härer W 1994 *IEEE Trans. Biomed. Eng.* **41**(4), 343–350. *The MIT-BIH Normal Sinus Rhythm Database* n.d.
*<http://www.physionet.org/physiobank/database/nsrdb/>
- Van-Trees H 2001 *Detection, Estimation, and Modulation Theory. Part I* John Wiley & Sons.
- Wan X, Iwata K, Riera J, Kitamura M & Kawashima R 2006 *Clinical Neurophysiology* **117**(3), 681–692.
*<http://dx.doi.org/10.1016/j.clinph.2005.07.025>
- Widrow B, Glover J, McCool J, Kaunitz J, Williams C, Hearn H, Zeidler J, Dong E & Goodlin R 1975 *Proc. IEEE* **63**(12), 1692–1716.